Experimental Characterization of a Novel Energy-efficient Integrated Microwave Photonics Modulator

Iterio Degli-Eredi* and Martijn J. R. Heck
Aarhus Universitet - Department of Engineering, Finlandsgade 22, 8200 Aarhus, Denmark
**e-mail: ideglieredi@eng.au.dk*

ABSTRACT

We design and experimentally characterize a novel microwave (MW) photonics ring modulator based on waveguide-resonator coupling modulation. The experiments reveal that at MW frequencies corresponding to the FSR of the ring or integer multiples thereof, the resonant device generates 10 to 19 times higher MW output power than the equivalent standard Mach-Zehnder modulator, thus showing our resonant modulator paves the way for energy-efficient and low driving MW power operation. Moreover, as this resonant enhancement occurs over a bandwidth of 2 to 3 GHz, our modulator has the potential to be implemented as a key element in the upcoming microwave and millimeter wave bands of 5G networks. Finally, the device solely consists of standard building blocks provided by the multi-project wafer run of the SMART Photonics foundry, thus showing it can be fabricated in a relatively mature photonics integration process.

Keywords: Microwave Modulators, Ring Resonators, Indium Phosphide, Microwave Photonics, Integrated Microwave Photonics

1 INTRODUCTION

In order to meet the increasingly high demand of bandwidth in optical telecommunication networks, there is considerable interest in improving the speed, power consumption and footprint of MW electro-optic modulators (EOMs) through photonic integration [1], [2]. One photonic integration material platform that can be used for on-chip MW modulation, but also amplification and lasing, and where the foundry process technology has already reached a certain level of maturity in terms of scalability, reproducibility and yield, is indium phosphide (InP) [3], [4]. However, foundry based InP modulators can only efficiently operate at MW frequencies lower than 15 GHz while upcoming telecommunication networks operate at frequencies far beyond 15 GHz such as the millimeter wave bands of 5G networks [4], [5]. And when using EOMs that rely on the Pockels effect, long modulator lengths or high driving voltages (i.e. high driving MW powers) are required for efficient operation [6], [4]. To tackle these issues, one can utilize the resonant enhancement in cavities, which has already been demonstrated in silicon ring modulators [7]. In addition, waveguide-resonator coupling modulation in ring modulators has proven to be more energy efficient than modulating the refractive index in the ring cavity [8], [9]. As such, we propose a novel MW ring modulator based on waveguide-resonator coupling modulation which will be described and experimentally characterized in the next section.

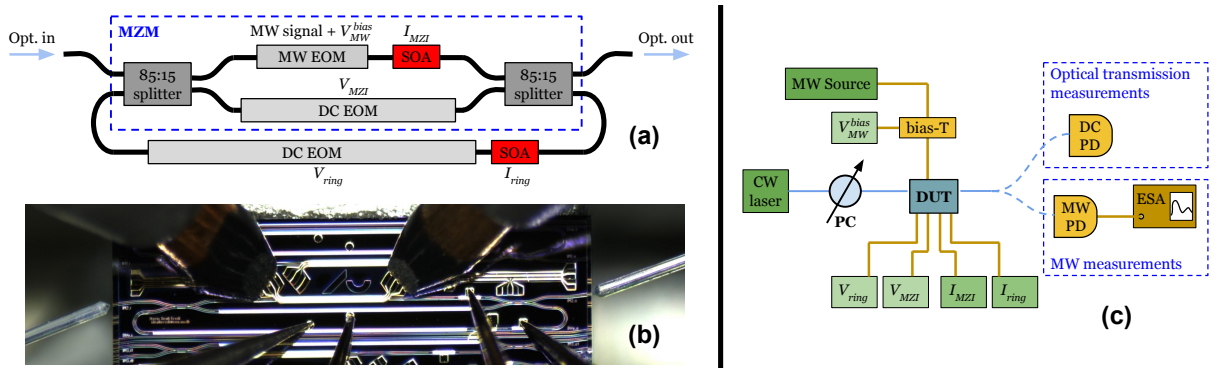

Figure 1. (a) Schematic of the ring resonator MW modulator. (b) Microscope image of the fabricated modulator with DC/MW probes and edge coupled fibers. (c) Measurement setup to obtain either the optical transmission or the MW response.

2 DESCRIPTION OF THE MODULATOR AND EXPERIMENTAL CHARACTERIZATION

2.1 Modulator principle and measurement setup

The device we consider is illustrated in Fig. 1(a): it is a ring resonator whose coupling section is a Mach-Zehnder modulator (MZM) that contains the MW EOM (length $L_{MW} = 950$ µm). The semiconductor optical

The research is supported by the Aarhus University Research Foundation AUFF, through a Lektor Starting Grant.

amplifiers (SOAs) in the MZM and ring arm are meant to compensate the insertion and ring losses respectively (the SOAs both have a length of $L_{SOA} = 200$ µm). The DC EOM in the MZM (length $L_{EOM}^{MZI} = 2.5\,\mathrm{mm}$) will be used to achieve critical coupling while the DC EOM in the ring arm (length $L_{EOM}^{ring} = 3\,\mathrm{mm}$) is meant to bias the device near resonance for a given wavelength. Finally, the splitters are 85:15 couplers (85% cross and 15% bar). The length of the connecting waveguides between the modulators and SOAs is chosen in such a way as to obtain an FSR close to 10 GHz. The device, along with some test structures, has been fabricated by the multi-project wafer (MPW) services of the SMART Photonics InP foundry and is depicted in Fig. 1(b). An external continuous-wave (CW) laser (Agilent 81600B) with polarization controller (PC) is edge coupled to the modulator, as seen in Fig. 1(c). We then either measure the transmitted optical power with an Agilent 81633A DC photodiode (PD) or, in case of MW measurements, retrieve the output MW signal from the external New Focus Model 1024 12-ps MW PD and measuring it with the R&S FSV30 electrical spectrum analyzer (ESA).

The resonant enhancement in the device can be explained as follows: during the first roundtrip, light from the CW laser with optical frequency f_c is modulated by the MW signal with frequency f_{MW} in the MZM and as a result, new frequencies $f_c + kf_{MW}$, with k integer, are generated. Via the ring waveguide, this modulated signal is fed back in the MZM, where also a 'new' unmodulated wave of the laser signal will enter of which the modulation will again generate a set of frequencies $f_c + kf_{MW}$. If these frequencies overlap in phase with the spectral content of the modulated signal from the previous roundtrip, the $f_c + kf_{MW}$ frequencies and thus the modulated signal will be resonantly enhanced - and this for all subsequent roundtrips. We expect the strongest MW response to happen when the device is tuned near resonance for a certain laser wavelength, and when the frequency f_{MW} of the MW signal is close to the FSR of the ring, thus resonantly enhancing the $f_c + kf_{MW}$ frequencies (where dispersion will ultimately put a limit on the maximally attainable k).

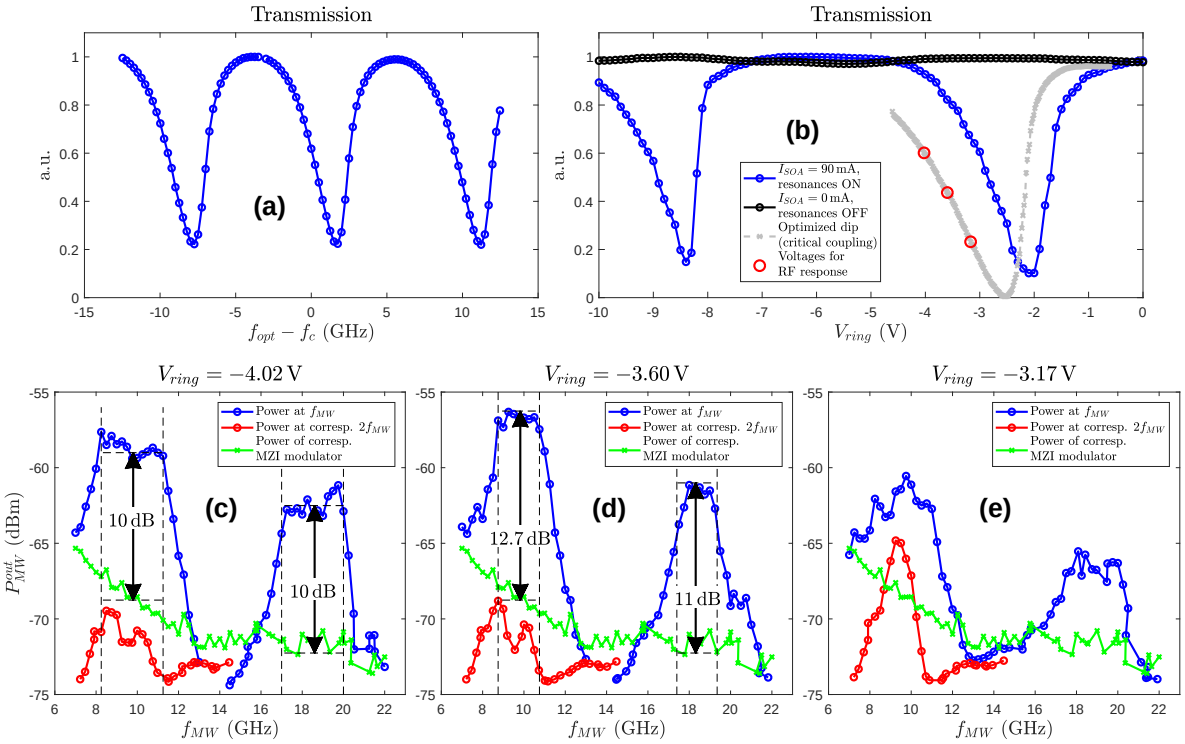

Figure 2. (a) Normalized transmission as a function of the optical frequency. (b) Normalized transmission as a function of V_{ring} (blue) together with the shape of the dip when critical coupling is achieved (grey) as well as the voltages chosen for the MW characterization (red). We also show the normalized transmission of the equivalent stand-alone MZM (black). In (c)-(e), the output MW power as a function of f_{MW} is plotted (blue) at the chosen V_{ring} values from (b) as well as the generated MW power at the corresponding $2f_{MW}$ (red). The data in (c)-(e) is compared with the generated MW power of the equivalent stand-alone MZM (green).

2.2 Measurement strategy and results

Before we experimentally characterize the MW response of the fabricated modulator, we first measure the transmission of the modulator as a function of the optical frequency of the CW laser plotted in Fig. 2(a), showing an FSR of 9.5 GHz. Then we optimize the modulator towards resonance and critical coupling. We fix the wavelength of the CW laser at $\lambda_0 = 1550\,\mathrm{nm}$ and keep the laser output power at a relatively low value of $P_0 = 5\,\mathrm{mW}$ to minimize the effect of optical nonlinearities in the ring. We set the DC voltages at $V_{MW}^{bias} = -4\,\mathrm{V}$ and $V_{MZI} = -6\,\mathrm{V}$, while the DC currents for the SOAs are set at $I_{MZI} = 5\,\mathrm{mA}$ and $I_{ring} = 90\,\mathrm{mA}$ (Fig.

1(a)), and we measure the optical output power as a function of V_{ring}, plotted in blue in Fig. 2(b) where the dips in the transmission indicate the cavity resonances. We then optimize the resonance located at $V_{ring} = -2.10\,\mathrm{V}$ towards critical coupling and find critical coupling is obtained for $V_{MZI}^{cc} = -4.17\,\mathrm{V}$ while the resonance is slightly shifted to $V_{ring}^{res} = -2.61\,\mathrm{V}$. Around the resonance, we choose a set of V_{ring} voltages where the RF response is characterized (red on Fig. 2(b)).

We now apply a MW signal of $16.5\,\mathrm{dBm}$ (from a R&S SMF100A MW signal generator) to the MW input of the MW EOM and sweep its frequency f_{MW} between $7\,\mathrm{GHz}$ and $22\,\mathrm{GHz}$ while we measure the MW output power at f_{MW} and $2f_{MW}$ on the ESA (see Fig. 1(c)). In Figs. 2(c)-(e), we show the MW response at $V_{ring} = -4.02\,\mathrm{V}$, $V_{ring} = -3.60\,\mathrm{V}$ and $V_{ring} = -3.17\,\mathrm{V}$ respectively. Figs. 2(c)-(e) clearly show resonant enhancement for MW frequencies around $f_{MW} = 9.5\,\mathrm{GHz}$ and $f_{MW} = 19\,\mathrm{GHz}$ which nicely overlaps with, respectively, one and two times the resonator's FSR of $9.5\,\mathrm{GHz}$. Another interesting observation is the fact that changing the bias voltage changes the shape of the resonant peaks: one can choose to maximize either the bandwidth of the peaks (Fig. 2(c) - at $f_{MW} = 9.5\,\mathrm{GHz}$, we obtain an MW power around $-59.0\,\mathrm{dBm}$ over a bandwidth of $3\,\mathrm{GHz}$) or the enhancement of the MW output power (Fig. 2(d) - at $f_{MW} = 9.5\,\mathrm{GHz}$, we obtain an MW power around $-56.3\,\mathrm{dBm}$ over a bandwidth of $2\,\mathrm{GHz}$). One can also opt to maximize the MW power of the generated second harmonic as Fig. 2(e) shows. Although the overall generated MW power of the second harmonic is still relatively low, the modulator under these bias conditions has the potential to be used as an electro-optic MW frequency multiplier after a further set of optimizations.

To check how well the resonant modulator performs as compared to the equivalent stand-alone MZM, we keep $I_{MZI} = 5\,\mathrm{mA}$ but turn off the SOA in the ring (i.e. $I_{ring} = 0\,\mathrm{mA}$). This ensures most of the light entering the ring waveguide is absorbed by the ring SOA and resonant enhancement is prevented. This is clear from the absence of resonance dips in its transmission spectrum plotted in black in Fig. 2(b). The MW response of this MZM, when excited with the same input MW signal with which the resonant modulator was excited, is plotted on Figs. 2(c)-(e) in green. Clearly, no resonant enhancement takes place in this device and as f_{MW} increases, the performance goes down due to the increasing MW losses in the coplanar waveguide of the MW EOM. When the resonant modulator is biased at "maximal enhancement" or where $V_{ring} = -3.60\,\mathrm{V}$ (Fig. 2(d)), the resonant modulator yields up to 19 times higher MW power for $f_{MW} = 9.5\,\mathrm{GHz}$ and $f_{MW} = 19\,\mathrm{GHz}$[1] than the stand-alone MZM. Even if we bias the resonant modulator at "wide bandwidth" or where $V_{ring} = -4.02\,\mathrm{V}$ (Fig. 2(c)), the modulator still generates a 10 times higher MW output signal.

3 CONCLUSIONS

While traditional MZMs fabricated in InP MPW runs cannot operate efficiently beyond a MW frequency of $15\,\mathrm{GHz}$ and require high driving MW powers, our novel integrated InP ring modulator has alleviated both issues by relying on both waveguide-resonator coupling modulation and resonantly enhancing the optical sidebands generated by the MW modulation and consequently the modulation depth and output MW power. We experimentally demonstrated that output MW power enhancements of 10 to 19 can be achieved at the resonances as compared to the stand-alone MZM, thus indicating the same modulation depth can be achieved at far lower driving MW powers. This not only happens for $f_{MW} = 9.5\,\mathrm{GHz}$ corresponding to the ring's FSR, but also beyond the MW EOM's bandwidth of $15\,\mathrm{GHz}$, namely twice the ring's FSR equal to $f_{MW} = 19.0\,\mathrm{GHz}$. On top of that, the enhancement around these resonances happen over a bandwidth of 2 to $3\,\mathrm{GHz}$, a feature that will be useful for the high frequency 5G bands below $40\,\mathrm{GHz}$ in Europe and elsewhere that require a bandwidth of up to 3 to $4\,\mathrm{GHz}$ [5]. Finally, the modulator only uses building blocks provided by the SMART Photonics MPW, thus showing the device can be fabricated in a relatively mature photonics integration process.

REFERENCES

[1] C. Wang et al., "Integrated lithium niobate electro-optic modulators operating at CMOS-compatible voltages," Nature, vol. 562, pp. 101–104, 2018.

[2] R. A. Griffin, S. K. Jones, N. Whitbread, S. C. Heck, and L. N. Langley, "InP Mach-Zehnder Modulator Platform for 10/40/100/200-Gb/s Operation", IEEE JSTQE, vol. 19, no. 6, pp. 158-166, November 2013.

[3] M. Smit et al., "An introduction to InP-based generic integration technology," Semicond. Sci. Technol., vol. 29, no. 8, pp. 083001, 2014.

[4] "Multiproject wafers," http://www.jeppix.eu/multiprojectwafers/, website visited in January 2019.

[5] "5G Frequency Bands," https://www.everythingrf.com/community/5g-frequency-bands, 2018, website visited in January 2019.

[6] R. Amin, J. B. Khurgin, and V. J. Sorger, "Waveguide-based electro-absorption modulator performance: comparative analysis," Opt. Express, vol. 26, no. 12, pp. 15445-15470, June 2018.

[7] J. Müller et al., "Optical Peaking Enhancement in High-Speed Ring Modulators," Sci Rep., vol. 4, pp. 6310, September 2014.

[8] W. M. J. Green, R. K. Lee, G. A. DeRose, A. Scherer, and Amnon Yariv, "Hybrid InGaAsP-InP Mach-Zehnder Racetrack Resonator for Thermooptic Switching and Coupling Control," Opt. Express, vol. 13, no. 5, pp. 1651–1659, March 2005.

[9] W. D. Sacher et al., "Coupling modulation of microrings at rates beyond the linewidth limit," Opt. Express, vol. 21, no. 8, pp. 9722–9733, April 2013.

1. For MW output powers below $-71\,\mathrm{dBm}$, the ESA measurements are highly affected by noise. We expect the actual output MW power of the stand-alone MZM around $f_{MW} = 19\,\mathrm{GHz}$ to be lower and therefore the enhancements higher than indicated on Figs. 2(d).